Production and characterization of a SARS-CoV-2 nucleocapsid protein reference material

Stocks, Bradley B.; Thibeault, Marie-Pier; L'Abbé, Denis; Stuible, Matthew; Durocher, Yves; Melanson, Jeremy E.

Publisher's version / Version de l'éditeur:
https://doi.org/10.1021/acsmeasuresciau.2c00050
ACS Measurement Science Au, 2, 6, pp. 620-628, 2022-09-02

ACS MEASUREMENT SCIENCE Au
AN OPEN ACCESS JOURNAL OF THE AMERICAN CHEMICAL SOCIETY

pubs.acs.org/measureau

Article

Production and Characterization of a SARS-CoV-2 Nucleocapsid Protein Reference Material

Bradley B. Stocks,* Marie-Pier Thibeault, Denis L'Abbé, Matthew Stuible, Yves Durocher, and Jeremy E. Melanson

Cite This: *ACS Meas. Sci. Au* 2022, 2, 620–628

Read Online

ACCESS | Metrics & More | Article Recommendations | Supporting Information

ABSTRACT: Rapid antigen tests have become a widely used COVID-19 diagnostic tool with demand accelerating in response to the highly contagious SARS-CoV-2 Omicron variant. Hundreds of such test kits are approved for use worldwide, predominantly reporting on the presence of the viral nucleocapsid (N) protein, yet the comparability among manufacturers remains unclear and the need for reference standards is recognized. To address this lack of standardization, the National Research Council Canada has developed a SARS-CoV-2 nucleocapsid protein reference material solution, NCAP-1. Reference value determination for N protein content was realized by amino acid analysis (AAA) via double isotope dilution liquid chromatography−tandem mass spectrometry (LC-ID-MS/MS) following acid hydrolysis of the protein, in conjunction with UV spectrophotometry based on tryptophan and tyrosine absorbance at 280 nm. The homogeneity of the material was established through spectrophotometric absorbance readings at 280 nm. The molar concentration of the N protein in NCAP-1 was 10.0 ± 1.9 μmol L^{-1} (k = 2, 95% confidence interval). Reference mass concentration and mass fraction values were subsequently calculated using the protein molecular weight and density of the NCAP-1 solution. Changes to protein higher-order structure, probed by size-exclusion liquid chromatography (LC-SEC) with UV detection, were used to evaluate transportation and storage stabilities. LC-SEC revealed nearly 90% of the N protein in the material is present as a mixture of hexamers and tetramers. The remaining low molecular weight species (<30 kDa) were interrogated by top-down mass spectrometry and determined to be autolysis products homologous to those previously documented for N protein of the original SARS-CoV [*Biochem. Biophys. Res. Commun.* **2008**t, *377*, 429−433].

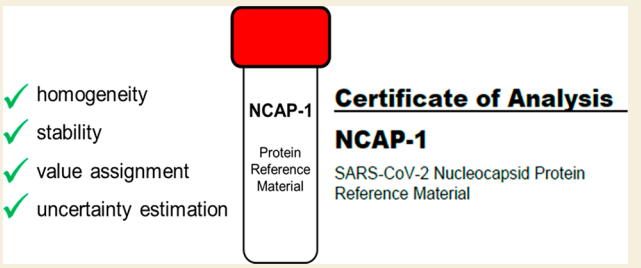

KEYWORDS: *COVID-19, SARS-CoV-2, nucleocapsid protein, reference materials, isotope dilution*

INTRODUCTION

The ongoing COVID-19 pandemic is caused by the SARS-CoV-2 virus, which has infected over 540 million people worldwide.[1] Multiple vaccines have been developed and deployed with unprecedented speed while providing excellent protection from serious disease. Several approved vaccines elicit an immune response to the spike protein (S), the viral protein responsible for binding to human cell-surface receptors. Antibodies target multiple epitopes on S;[2,3] however, mutations can allow the virus to evade the immune response. The effect of these escape mutations has been observed by the recent emergence of the Omicron B.1.1.529 variant[4] (and multiple subvariants), which is dramatically more transmissible than previous variants and now accounts for the vast majority of infections. The steep increase in transmission during the Omicron wave has forced health agencies to modify their COVID testing strategies.

While RT-PCR remains the definitive method to diagnose infection by detecting viral RNA, the associated logistics render widespread testing unrealistic. To facilitate mass testing efforts, multiple rapid antigen tests have been approved,[5−7] and their use has increased exponentially in response to the most recent wave of infections. Such tests can be performed at home without the need for specialized training and rely on a visual readout. The vast majority of antigen tests detect the SARS-CoV-2 nucleocapsid (N) protein due to its abundance in circulation early during infection.[8] Operating on principles similar to those of antigen tests, serology (i.e., antibody) tests report on the presence of anti-S and/or anti-N antibodies (Abs) in patient serum. The presence of anti-N Abs can distinguish those who have been previously infected from vaccinated yet uninfected individuals, facilitating potential large-scale surveillance studies to estimate overall infection levels in highly vaccinated populations.[9,10]

Received: July 19, 2022
Revised: August 22, 2022
Accepted: August 23, 2022
Published: September 2, 2022

Ensuring comparability between test kits from various manufacturers is essential yet often difficult due to intellectual property concerns regarding antigen/Ab identities and structures. Reference materials support measurement accuracy and enhanced reliability, and thus can be valuable tools to assess comparability between test kits. We recently characterized a spike protein reference material[11] for use in various applications including lateral flow assays. With regard to nucleocapsid, production of recombinant protein has been reported using a variety of methods in different cell types, including bacterial, insect, and mammalian cells.[12−15] Such diverse approaches generate products with variable characteristics, including differences in post-translational modification and oligomeric status, which will likely impact their performance in different assays. To further address the lack of standardization, we have developed a SARS-CoV-2 N protein reference material, NCAP-1, based on the native viral N sequence (with C-terminal affinity tags added for purification) expressed in CHO cells. Notably, despite the absence of an N-terminal signal peptide (secretion signal), N is spontaneously released into CHO cell culture supernatants, thus facilitating purification compared to other production methods. This material is designed to serve as a positive control for antigen tests, and has already been shown to be valuable as an antigen source for ELISA-based Ab assays.[16] The production and characterization of this protein reference material should dramatically increase confidence and harmonization in SARS-CoV-2 immunological testing results.

MATERIALS AND METHODS

Chemicals and Standards

NRC certified reference materials (CRMs) ALEU-1 (leucine), APHE-1 (phenylalanine), and APRO-1 (proline) were used as primary standards for AAA.[17] The amino acid CRMs were purity assigned by quantitative ^{1}H NMR traceable to NIST potassium hydrogen phthalate (SRM 84L). The corresponding isotope-labeled amino acids were sourced from Cambridge Isotope Laboratories (CIL, Tewksbury, MA): [$^{13}C_6$]-leucine, [ring-$^{13}C_6$]-phenylalanine, and [$^{13}C_5$]-proline. NIST recombinant humanized IgG1κ monoclonal antibody reference material (NISTmAb, RM 8671) was purchased from NIST (Gaithersburg, MD). Amino acid analysis grade 6 M hydrochloric acid, Dulbecco's phosphate buffered saline, arginine, and chymotrypsin were obtained from Sigma (Oakville, ON). Acetonitrile, formic acid, ammonium acetate, Tris-HCl, and NaCl were purchased from Fisher Scientific (Nepean, ON). Glacial acetic acid was from ACP Chemicals (Montreal, QC) and sequencing grade trypsin was from Promega (Madison, WI).

Protein Production and Reference Material Preparation

Recombinant N protein was produced and purified as described previously.[16] Briefly, a CHO codon-optimized sequence encoding the native SARS-CoV-2 reference strain N protein fused to C-terminal FLAG-dual-Strep-His affinity tags was cloned into the pTT5 expression vector. The protein was produced by transient gene expression (TGE), by PEI-mediated transfection of the pTT5-NCAP plasmid into CHO^{S5E1} cells growing in suspension culture in chemically defined media. Culture supernatant harvested following a 7-day fed-batch process was purified by sequential IMAC and Strep affinity chromatography columns. The final product was formulated in 50 mM Tris, pH 8.0, containing 150 mM NaCl using a desalting column and stored at −80 °C. Prior to reference material bottling, the protein solution was thawed in a 25 °C water bath and diluted 1:3 with formulation buffer in a biosafety cabinet. The diluted solution was dispensed in 0.4 mL aliquots into sterile 2 mL cryovials, labeled, and stored at −80 °C.

NCAP-1 Sequence Analysis by LC-MS/MS

Peptide Mapping and Host-Cell Protein Detection. NCAP-1 aliquots were digested overnight at 37 °C with trypsin (1:20 w/w) or chymotrypsin (1:50 w/w). Resultant peptides were separated on a 2.1 × 150 mm BEH130 C18 column (Waters, Milford, MA) with a water:acetonitrile gradient in the presence of 0.1% formic acid delivered by a Thermo Fisher Scientific Vanquish UHPLC (San Jose, CA). Eluting peptides were detected with an Orbitrap Fusion Lumos (ThermoFisher Scientific). The ESI needle voltage was held at +3600 V and the sheath, auxiliary, and sweep gas flows were 35, 10, and 2, respectively (arbitrary units). The ion transfer tube and vaporizer temperatures were set to 275 and 250 °C, respectively. Survey scans were acquired from m/z 350−1400 at 60 000 resolution and RF 30%. Fragment spectra were generated via CID (35% normalized CE) and detected in the ion trap. Data analysis proceeded in MaxQuant 1.6[18] employing the *Cricetulus griselus* Uniprot reference proteome database supplemented with the nucleocapsid protein sequence and those of common contaminants. Proteins detected by MS/MS with ≥3 unique peptides were considered positive identifications. Relative host-cell protein abundances were estimated using iBAQ[19] and are shown in Table S1.

Top-Down CID. Protein separation was achieved using a Waters BEH300 C4 column (2.1 × 50 mm). Survey scans were collected with the Orbitrap Fusion Lumos operating at 50 000 resolution over a 150−2000 m/z range. Fragment ions were generated via CID (30% CE) with detection in the Orbitrap at 15 000 resolution. Charge state distributions were deconvoluted with FreeStyle 1.7 software provided by the instrument manufacturer and UniDec,[20] and masses were tentatively matched (Δm < 5 ppm) to N protein fragments via ExPASy tool FindPept (https://web.expasy.org/findpept/). Sequences were confirmed by analyzing top-down CID fragment ion spectra with TopPIC.[21]

Amino Acid Analysis by LC-ID-MS/MS

Isotopically labeled amino acid ($^{13}C_6$-Leu, $^{13}C_6$-Phe, and $^{13}C_5$-Pro) stock solutions were prepared gravimetrically in ultrapure water and then combined as internal standards in mole fractions representing those in the NCAP-1 sequence to enable exact-matching isotope dilution (1:1 ratio). A corresponding blend of the natural amino acids (Leu, Phe, and Pro) and two blends bracketing the 1:1 ratio (0.5 and 1.5 ratio) were prepared as calibrants. Equal amounts of the internal standard were then spiked into each of the calibration blends and NCAP-1, followed by liquid phase acid hydrolysis in 6 M HCl. The solutions were incubated at 110 °C for 72 h to ensure complete peptide bond cleavage,[22,23] then equilibrated to ambient temperature. A 40 μL aliquot of each solution was diluted to 1 mL prior to LC-MS/MS analysis. NISTmAb RM 8671 was diluted 10-fold, spiked with ^{13}C-labeled amino acids, and hydrolyzed in parallel as a quality control sample.

Analyte separation was achieved on a Macherey-Nagel Nucleodur HILIC column (2.0 × 100 mm, 3.0 μm particle) thermostated at 35 °C. The mobile phase was delivered by an Ultimate 3000 UHPLC instrument (ThermoFisher Scientific), and isocratic elution proceeded with 10 mM ammonium acetate in 88% acetonitrile, adjusted to pH 3.5 with glacial acetic acid at 0.25 mL min^{-1}. Eluting amino acids from 4 μL injections were directed into the heated electrospray source of a Thermo Quantiva triple quadrupole MS instrument operating in multiple reaction monitoring (MRM) mode. Compound specific parameters were first optimized by infusing individual amino acid standards: ion transitions (Q1/Q3), collision energy (CE), and radio frequency (RF) values used are shown in Table S2. The ESI needle voltage was set to +4400 V and the sheath, auxiliary, and sweep gas flows were 25, 17, and 1, respectively (arbitrary units). The ion transfer tube and vaporizer temperatures were set to 325 and 280 °C, respectively. Peak areas were extracted using Xcalibur software from the instrument manufacturer.

Quantitation of each amino acid in the sample (w_A) was achieved using the following quadruple isotope dilution equation:[24]

https://doi.org/10.1021/acsmeasuresciau.2c00050
ACS Meas. Sci. Au 2022, 2, 620−628

$$w_A = w_{A^*} \cdot \frac{m_2 m_3 r_4 + m_1 m_3 r_5 + m_1 m_2 r_6}{m_1 r_4 + m_2 r_5 + m_3 r_6} \cdot \frac{m_{B(AB)}}{m_{A(AB)}}$$

$$m_{A^*-i} = \frac{m_{A^*(A*B-i)}}{m_{B(A*B-i)}}$$

$$r_4 = (r_{AB} - r_{A*B-1}) \cdot (r_{A*B-2} - r_{A*B-3})$$

$$r_5 = (r_{AB} - r_{A*B-2}) \cdot (r_{A*B-3} - r_{A*B-1})$$

$$r_6 = (r_{AB} - r_{A*B-3}) \cdot (r_{A*B-1} - r_{A*B-2}) \quad (1)$$

where A represents the analyte in the sample, A* the primary standard (natural amino acid), B the internal standard (labeled amino acid), A*B the calibration blend, and AB the sample blend. Symbols w_x denote the mass fraction of X in the solution (X = A, A*, or B), $m_{x(xy)}$ is the mass of solution x to prepare the blend xy, and r_x is the measured isotope amount ratio of x. Validation of this technique has been demonstrated in interlaboratory comparisons[25−27] and has facilitated the development of multiple protein reference materials.[11,28,29]

Ultraviolet−Visible Spectrophotometry

Protein concentration in NCAP-1 was determined using a NanoDrop One^c (ThermoFisher Scientific) UV−visible spectrophotometer at 280 nm. Instrument performance was verified through analysis of NISTmAb RM 8671 and a Pierce bovine serum albumin standard. The instrument was blanked with NCAP-1 formulation buffer. A volume of 2 μL of NCAP-1 solution was pipetted onto the pedestal, and the pathlength was set to 1 mm. Pathlength uncertainty was determined through analysis of the Thermo Fisher PV-1 solution. The protein concentration was calculated via the Beer−Lambert equation using an extinction coefficient of 59 380 M^{-1} cm^{-1},[30] predicted from the N protein amino acid sequence (Figure S1).

Size Exclusion Chromatography

Liquid chromatography was performed on an Agilent 1290 UPLC instrument (Santa Clara, CA) equipped with a Superdex 200 Increase 5/150 column (Cytiva, Vancouver, BC). Instrument and column performance was confirmed with the Cytiva high molecular weight protein standard mix and NISTmAb RM 8671. The autosampler was maintained at 10 °C. A volume of 10 μL of NCAP-1 (~5 μg N protein) was injected onto the column and eluted at 0.25 mL min^{-1} with DPBS supplemented with 0.2 M arginine, pH 7.4. Solvent was directed into the flow cell of the Agilent 1290 diode array detector operating at 280 nm with 1.2 nm resolution. Data analysis was done with ChemStation software provided by the instrument manufacturer. Column void volume was measured with blue dextran, and protein partition coefficients were calculated using eq 2:

$$K_{av} = \frac{V_e - V_0}{V_c - V_0} \quad (2)$$

where V_e and V_0 are the elution volumes of the protein analyte and blue dextran, respectively, and V_c is the SEC column volume. Peak fitting was done via Gaussian decomposition with OriginPro 2016.

RESULTS AND DISCUSSION

NCAP-1 Sequence Determination

Liquid chromatography MS after proteolysis resulted in ~95% sequence coverage (Figure S1). Peptide mapping indicated the initiator Met residue was cleaved during expression and the resultant N-terminus (Ser2) was acetylated. Identical N-terminal processing was observed in SARS-CoV N protein isolated both from patients[31] and from infected Vero E6 cells.[32] Initiator methionine cleavage of the SARS-CoV-2 N protein has not been widely reported in the literature; therefore, to facilitate comparisons with prior studies, the N-terminal serine in NCAP-1 is maintained as residue two.

Homogeneity of NCAP-1

Protein solutions are often highly uniform; however, heterogeneity can occur for a variety of reasons, i.e., inconsistent environmental conditions during the production process, temporal interaction between the sample and its container, and contamination. Further, changes to the protein higher-order structure may alter the readout of the chosen detection method. Therefore, a homogeneity assessment was performed using the molar protein concentration measured by UV−vis at 280 nm, and a corresponding uncertainty component was determined. Fifteen units were randomly selected from the fill batch, and each unit was analyzed in triplicate (Figure 1). The between unit variability was

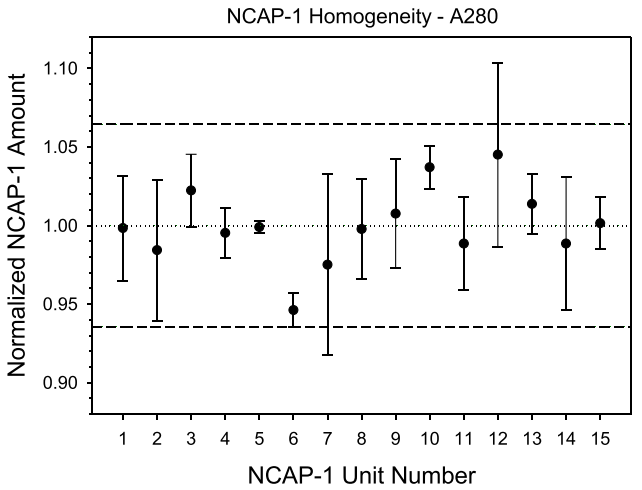

Figure 1. Normalized protein content in 15 randomly selected NCAP-1 units. Data points and error bars represent averages and standard deviations, respectively, of triplicate technical replicates. Dotted line is the average molar concentration determined by A_{280} and dashed lines indicate expanded uncertainty (k = 2, 95% CI).

determined using the Bayesian analysis of variance (ANOVA) with priors set for the mean, the scale and the half-Cauchy parameters. The model was fit to data using Monte Carlo with R package *rjags*, and the resulting homogeneity uncertainty (u_{hom}) with 95% confidence interval was 0.12 μmol L^{-1}. This uncertainty due to inhomogeneity was considered negligible when compared to the combined NCAP-1 uncertainty (0.96 μmol L^{-1}),[33] hence the material was deemed homogeneous.

Preservation of the native higher-order (tertiary, quaternary) structure is a critical factor for protein reference materials. The N protein natively forms homodimers, which then further associate into larger, functional oligomers such as tetramers and hexamers.[34,35] The N protein has also been shown to undergo spontaneous cleavage, and the presence of these truncated forms could have effects on assays employing NCAP-1 as a reagent. Therefore, the relative amount of N protein oligomers (namely, hexamers and tetramers) in NCAP-1 was assessed by LC-SEC-UV on the same 15 units. The main elution peak ostensibly contained a mixture of N protein hexamers (~300 kDa) and tetramers (~200 kDa) while two low molecular weight species (~30 and ~18 kDa) were also observed (Figure 2). SEC-UV peak area measurements revealed that NCAP-1 consists mostly of N oligomers (88%) along with the two low molecular weight species (9% and 3%, respectively). Between vial repeatability standard

https://doi.org/10.1021/acsmeasuresciau.2c00050
ACS Meas. Sci. Au 2022, 2, 620−628

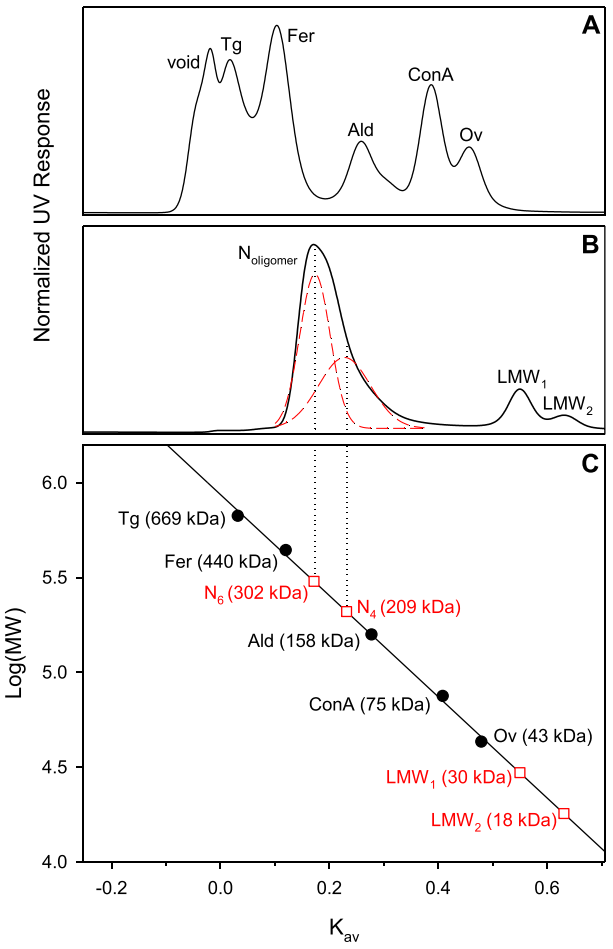

Figure 2. Size exclusion UV chromatograms of (A) molecular weight standard protein mix and (B) NCAP-1. Void volume was determined from elution of blue dextran. Standard protein mix consists of thyroglobulin (Tg), ferritin (Fer), aldolase (Ald), conalbumin (ConA), and ovalbumin (Ov). Panel (C) shows molecular weight calibration of the SEC column and calculated values for sample peaks in (B). Red dashed lines in panel (B) result from Gaussian decomposition and correspond to hexamers (N_6) and tetramers (N_4). K_{av} values calculated using eq 2.

deviations were <1%; however, a full uncertainty estimation was not performed and thus the structural heterogeneity values determined by SEC-UV were included as information values only. No significant difference in oligomer abundance was detected between units (Figure S2), further suggesting a homogeneous preparation.

NCAP-1 Stability

The SARS-CoV-2 N protein self-assembles into dimers which then further oligomerize into tetramers and hexamers. We therefore assessed the short-term and freeze−thaw stability of the N protein oligomeric distribution in NCAP-1 by size-exclusion chromatography. Figure 2 shows the SEC column molecular weight calibration and the elution profile of NCAP-1 stored at −80 °C. The asymmetry in the main N protein peak is suggestive of heterogeneity in the oligomeric state, and Gaussian decomposition revealed a probable mixture of hexamers (N_6) and tetramers (N_4), consistent with previous reports.[35,36] Consideration of alternative potential oligomers, i.e., pentamers and trimers, did not significantly improve the fitting and were therefore excluded from further analyses. We note here that the Gaussian deconvolution was performed for information purposes only and that the total area of the oligomer elution peak was utilized as a surrogate for native N protein during the NCAP-1 stability assessment. However, it is acknowledged that alterations to the oligomeric distribution may expose or occlude binding epitopes, potentially affecting the readout of various Ab assays. Changes to the hexamer−tetramer distribution were observed after extended storage (>1 day) outside of the freezer (Figure S3), thus explicit instructions regarding storage and use are included in the certificate of analysis which accompanies the reference material.[37] The two low molecular weight (LMW) peaks in the chromatogram, corresponding to 30 kDa and 18 kDa species, are discussed in a subsequent section.

The short-term stability was investigated to assess potential conditions encountered during transport and brief storage, as well as during sample preparation and analysis. Using an isochronous approach, duplicate samples were incubated at each of four temperatures (+40, +20, +4, and −20 °C) for each of three time points (1, 7, and 14 days) and then analyzed with reference to samples held at −80 °C. As shown in Figure 3A,

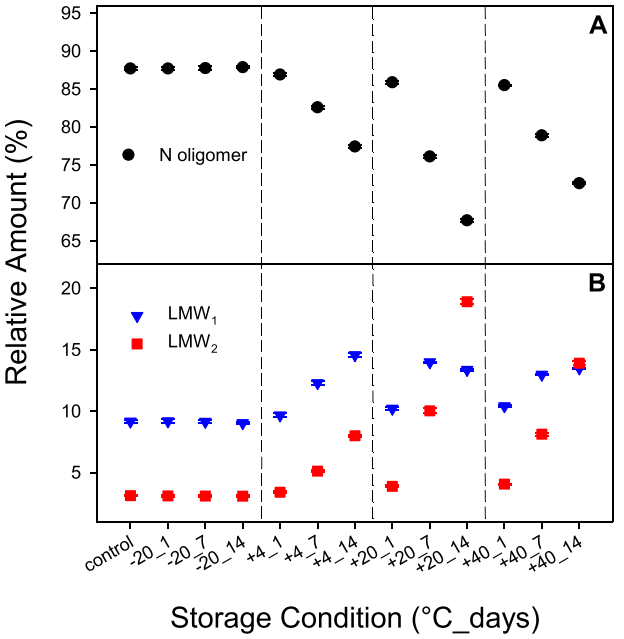

Figure 3. Normalized amount of (A) total nucleocapsid oligomer (hexamers and tetramers) and (B) low molecular weight species in NCAP-1 under various storage conditions. Values result from triplicate measurements of two units per condition. Data points and error bars represent averages and standard deviations, respectively.

no significant changes in protein size heterogeneity were observed when the reference material (RM) was stored at −20 °C. Small decreases (<2%) in the relative amount of N oligomers were apparent after 1 day of storage outside of the freezer, and the decrease in the oligomer peak dramatically accelerated with both storage time and temperature. In all cases, the loss of N oligomer was accompanied by concomitant increases in the two LMW species (Figure 3B). At elevated temperatures (+20 °C and +40 °C), the formation of the 30 kDa species plateaued after 7 days while the formation of the 18 kDa species continued to increase. This behavior was posited to result from further degradation of the 30 kDa

https://doi.org/10.1021/acsmeasuresciau.2c00050
ACS Meas. Sci. Au 2022, 2, 620−628

species, potentially due to additional cleavage after Lys388 or Lys389 (Table 1, Figure S4).

Table 1. NCAP-1 Autolysis Product Identifications

peak number	deconvoluted mass (g/mol)	theoretical mass (g/mol)[a]	NCAP-1 residues	cleavage sequence
1	4169.97	4169.97	2−40	KQR | RPQ
2	3885.83	3885.81	2−38	RSK | QRR
3	3670.68	3670.68	2−36	GAR | SKQ
4	9071.23	9071.23	381−463	ETQ | ALP
5	7564.37	7564.37	394−463	TVT | LLP
6	8249.74	8249.74	388−463	RQK | KQQ
7	8121.65	8121.65	389−463	QKK | QQT
main NCAP-1 elution peak	19917.9	19917.9	2−185	SSR | SSS
	30437.8	30437.6	186−463	
	20578.6	20578.6	2−191	RSR | NSS
	29776.8	29776.9	192−463	
	46183.8	46183.2	41−463	KQR | RPQ
	50337.9	50337.5	2−463	intact N

[a]Values for peaks 1−7 are monoisotopic masses; main NCAP-1 peak species are average masses.

The stability of NCAP-1 was evaluated using the results of the isochronous study described above. A simple first-order degradation with a three-parameter super-Arrhenius model was fitted to the data to make predictions for potential degradation of NCAP-1 after: (1) 2 days at +30 °C to simulate a significant shipping delay as the material is shipped on dry ice and (2) 1 year storage at −20 °C. These short- and long-term uncertainty components were combined into the final stability uncertainty for NCAP-1 (Table 2). The estimates are

Table 2. Uncertainty Components of Reference Values for NCAP-1

substance	$U_{k=2}$	u_c	u_{char}	u_{hom}	U_{stab}
SARS-CoV-2 nucleocapsid protein molar concentration (μmol L^{-1})	1.9	1.0	0.3	0.0	0.9
SARS-CoV-2 nucleocapsid protein mass concentration (mg mL^{-1})	0.09	0.05	0.02	0.00	0.05

conservative projections of possible instability, especially at −20 °C, as the actual long-term stability under such conditions has not yet been rigorously assessed. Storage in a freezer at approximately −80 °C is therefore recommended.

Finally, NCAP-1 freeze−thaw (F/T) stability was assessed. Duplicate samples were subjected to 1, 2, 3, 5, or 10 F/T cycles, defined as ≥1 h incubation at ambient temperature followed by ≥2 h storage at −80 °C. Figure 4 shows that F/T cycles (≤10) had no significant effect on the relative amount of N oligomer or the hexamer−tetramer distribution. We note however that LC-SEC-UV reports only on the size heterogeneity of the material and results from alternative structural or functional methods may differ.

Low Molecular Weight Species Identification

Liquid chromatography SEC-UV revealed the presence of two low molecular weight species in NCAP-1 corresponding to ∼30 kDa (LMW_1) and ∼18 kDa (LMW_2), as mentioned

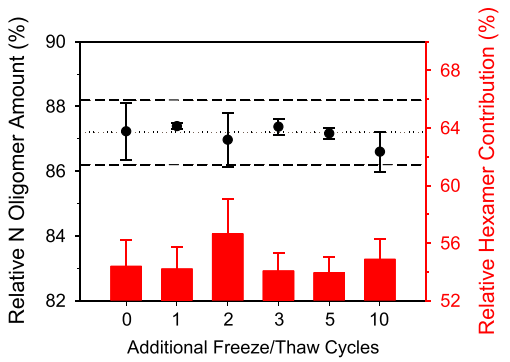

Figure 4. Freeze−thaw effects on protein size heterogeneity in NCAP-1. Left axis: Relative amount of N protein oligomer as a function of freeze−thaw cycle number. Right axis: Relative hexamer contribution to total N oligomer signal. Two NCAP-1 units were used for each condition and analyzed in triplicate. Data points and error bars represent averages and standard deviations, respectively. The average N oligomer values of the control samples (zero F/T cycles) ± 1% are indicated by the dotted and dashed lines, respectively, and are for visualization purposes only.

above. Truncated products were also observed by gel electrophoresis during production of the bulk N protein present in NCAP-1.[16] The sum of the two LMW species masses approximates the molar mass of the intact N monomer (50.3 kDa), suggesting a fraction of the N protein in NCAP-1 could have been cleaved. Given the rigorous characterization required for reference material production, this prompted further investigation.

The N protein binds to viral RNA to pack into the helical ribonucleocapsid complex but must unpack upon cellular uptake to liberate RNA for viral replication.[38] This dissociation may be facilitated via cleavage by cellular proteases[39,40] and/or (de)phosphorylation of serine residues.[41−43] Interestingly, prior work on the SARS-CoV N protein revealed spontaneous autolytic cleavage within the serine/arginine (SR)-rich region, even in the absence of proteases.[44] The SR-rich region is located within the disordered linker between the N- and C-terminal domains, is reported to be crucial for effective viral replication,[45] and is highly conserved within the SARS-CoV and SARS-CoV-2 N proteins.[42] To determine whether the LMW species we observed were due to cleavage events within the SR-rich region we subjected NCAP-1 to LC-MS/MS using a top-down approach.

The LC-MS chromatogram revealed multiple low-intensity peaks in addition to the main elution (Figure 5A). Deconvolution of the overlapping charge state distributions contained within the main elution peak revealed predominantly intact N protein as well as ∼10% phosphorylated N (Figure 5B). The phosphorylation was localized to Ser206, within the SR-rich region, from peptide mapping experiments (Figure S5), consistent with previous findings for both SARS-CoV[46] and -CoV-2.[41] No other phosphorylation sites were positively identified. Additional peaks in the deconvoluted mass spectrum were assigned to N protein fragments resulting from cleavage at two sites within the SR-rich region (C-terminal to R185 and R191), identical to the autolysis sites previously identified for the SARS-CoV N protein. This indicated that the LMW peaks observed by SEC-UV likely correspond to $N_{186-463}/N_{192-463}$ (∼30 kDa) and N_{2-185}/N_{2-191} (∼20 kDa).

https://doi.org/10.1021/acsmeasuresciau.2c00050
ACS Meas. Sci. Au 2022, 2, 620−628

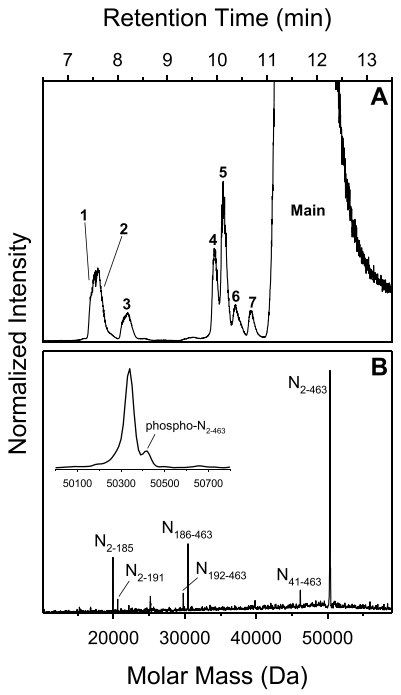

Figure 5. Denaturing LC-MS of NCAP-1 unit stored at −80 °C. (A) LC-MS chromatogram with main elution peak cropped to observe minor species. Peak numbering corresponds to that of Table 1. (B) Deconvoluted mass spectrum resulting from integration of main elution peak in panel (A). Peak labeling corresponds to N protein residue numbers. Inset shows zoom-in on intact N peak.

No detectable N- or O-linked glycans were observed in the NCAP-1 reference material. Notably, previous studies characterizing recombinant N protein produced in HEK293 and CHO cells have reported extensive N- and O-linked glycosylation, likely due to addition of an N-terminal signal peptide to the native N amino acid sequence to facilitate secretion into culture media.[12] This glycosylation is likely due to the protein being un-naturally directed into the mammalian cell secretory pathway by the signal peptide, and can result in masking of epitopes of anti-N antibodies induced by viral infection, rendering it a less effective antigen for serology assays.[47] The ability of CHO cells to release recombinant nucleocapsid into the culture supernatant despite the absence of secretion signal appears advantageous, facilitating purification yet avoiding extraneous post-translational modifications.

Additional very low molecular weight (vLMW, <10 kDa) species were identified via LC-MS which went undetected in the SEC-UV experiments. Seven distinct N protein cleavage products were measured: three N-terminal and four C-terminal fragments. As with the cleavages in the SR-rich linker region, five of the seven vLMW products result from cleavage within a basic region (Table 1). Each of these fragments was also observed to increase in prevalence with extended storage time at ambient temperature (Figure S4). The remaining vLMW species (peaks 4 and 5) correspond to C-terminal fragments resulting from cleavage after a polar residue (Q/T) and show no increase in formation as a function of incubation time. Interestingly, the cleavage of peak 5 is only 1 residue shifted from a cleavage product observed in N protein expression batches from *E. coli* and HEK293 cells.[40] While the apparent autolysis occurred largely in basic patches of the protein, peaks 4 and 5 more closely resemble fragments generated in vivo. Because there was no change in their abundance over 7 days at 20 °C and they both contain the C-terminal affinity tags of the NCAP-1 construct, we hypothesized that they were generated during protein expression and copurified with full-length N.

Overall, the LC-MS/MS results support the conclusion that the LMW species observed to increase both with storage time and temperature result from spontaneous cleavage within basic patches of the N protein. The autolysis sites within the SR-rich region of SARS-CoV-2 N detected in this work mirror those observed in the original SARS-CoV nucleocapsid protein.[44] Nonetheless, Figure 3 demonstrates that production of the LMW species can be controlled under proper storage and usage conditions.

Reference Value Assignment and Uncertainty Evaluation of NCAP-1

NCAP-1 is a reference material evaluated for nucleocapsid protein content. The reference value reported for N protein molar concentration is based on results from two orthogonal methods: UV−vis spectrophotometry and amino acid analysis ID-MS. Measurements were performed on the same 15 units used for the homogeneity assessment, in addition to a NISTmAb quality control sample. It should be noted that both UV−vis and AAA are nonselective techniques that report on the total amount of protein in the sample. We therefore assessed for the presence of host-cell proteins and using the iBAQ algorithm[19] within MaxQuant estimated their abundance to be approximately 0.5% of the total protein content (Table S1), reflective of the extensive purification during production of the bulk N protein material.[16] Because of the high purity of the RM and the large uncertainty associated with HCP amount estimation,[48] we did not perform an explicit impurity correction for the N protein concentration measurements. We did however include a corresponding type B component of 0.05 μmol L^{-1} into the uncertainty budgets for both the UV−vis and AAA measurements.

Absorbance readings were recorded on a microvolume spectrophotometer, which has been shown to result in <3% error for amino acid and nucleotide samples.[49] The average concentration of the 15 units was 9.6 ± 0.4 μmol L^{-1} (k = 1), with the characterization uncertainty incorporating the standard deviations of triplicate measurements and the pathlength error determined during instrument verification. A component reflecting the uncertainty in the extinction coefficient was also included, estimated from the bias in the NISTmAb standard measurement, as well as the HCP component discussed above. The total protein molar concentration determined by amino acid analysis following protein hydrolysis was 10.4 ± 0.3 μmol L^{-1} (k = 1), and the characterization uncertainty results almost entirely from the repeatability of the LC-MS isotope ratio measurements (Figure S6). The spread between the values reported by the two methods likely stems from the multiple N protein cleavage products in the material. These will contribute to the amino acid analysis result in the same manner as the intact N protein; however, they may not be accurately captured in the UV−vis experiment when using the extinction coefficient predicted for the full-length protein. Nonetheless, the concentrations from the two methods were consistent within the 95% CI and averaged to give a consensus value of 10.0 ± 0.3 μmol L^{-1} (k = 1) (Table 2). The characterization uncertainty from the consensus value was combined with the short-term and long-term stability uncertainties to give a final uncertainty of 1.9 μmol L^{-1} (k = 2, 95% CI) (Table 3). To

https://doi.org/10.1021/acsmeasuresciau.2c00050
ACS Meas. Sci. Au 2022, 2, 620−628

Table 3. Reference Values and Expanded Uncertainties (k = 2, 95% CI) for NCAP-1

substance	molar concentration (μmol L^{-1})	mass fraction (mg g^{-1})	mass concentration (mg mL^{-1})
SARS-CoV-2 nucleocapsid protein	10.0 ± 1.9	0.50 ± 0.09	0.50 ± 0.09

accommodate end-users working with mass concentrations, the molar concentration was converted using the average molar mass of the N protein (50 337 ± 1 g mol^{-1}) resulting in a value of 0.50 ± 0.09 mg L^{-1}. Finally, the density of the RM solution was measured as 1.01 ± 0.01 g mL^{-1} and used to calculate a mass fraction of 0.50 ± 0.09 mg g^{-1} nucleocapsid protein in NCAP-1.

Nucleocapsid as a Potential Subunit Vaccine Antigen

As the most abundant protein in SARS-CoV-2 virions, the nucleocapsid is an important target of antibodies induced during infection as well as being a frequent source of T-cell epitopes enabling cell-based immunity.[50,51] There is significant interest in augmenting efficacy of current spike-based vaccines by incorporating nucleocapsid, introduced via a viral vector[52] or as a purified protein.[53] Although our current work on NCAP-1 is intended exclusively to support its use as a reference material for diagnostic and serology assays, there is certainly potential for a similar antigen to be developed for inclusion in a next-generation SARS-CoV-2 vaccine formulation. In particular, the expression platform used for NCAP-1 production, i.e., CHO suspension culture, is compatible with biomanufacturing,[54] and the release of the protein from CHO cells without the addition of unwanted glycosylation facilitates downstream purification and would likely improve resemblance to the native protein found in SARS-CoV-2 virions relative to other production platforms.

CONCLUSIONS

Circulation of highly infectious SARS-CoV-2 variants have facilitated the persistence of the COVID-19 pandemic and reinforced the importance of rapid diagnostics and viral surveillance. To facilitate comparability between N protein antigen test kits, we have characterized a nucleocapsid protein reference material, NCAP-1. The reference material was determined to be homogeneous and sufficiently stable under shipping and storage conditions, and it demonstrated resistance to multiple freeze/thaw cycles. The material is envisaged to be used as a standard protein reagent for developing SARS-CoV-2 serological and antigen tests. NCAP-1 can also be used as a SI-traceable calibrator in the development of N protein quantitation assays.

ASSOCIATED CONTENT

Supporting Information

The Supporting Information is available free of charge at https://pubs.acs.org/doi/10.1021/acsmeasuresciau.2c00050.

Host-cell protein identifications; amino acid MS/MS parameters NCAP-1 peptide mapping; LC-SEC homogeneity; stability analysis of N oligomer distribution; temporal LMW species formation; phosphopeptide MSMS; LC-ID-MS/MS amino acid quantitation (PDF)

AUTHOR INFORMATION

Corresponding Author

Bradley B. Stocks − *Metrology, National Research Council Canada, Ottawa, ON K1A 0R6, Canada*; orcid.org/0000-0002-7265-9344; Phone: 613-993-4416; Email: bradley.stocks@nrc-cnrc.gc.ca

Authors

Marie-Pier Thibeault − *Metrology, National Research Council Canada, Ottawa, ON K1A 0R6, Canada*

Denis L'Abbé − *Human Health Therapeutics, National Research Council Canada, Montreal, QC H4P 2R2, Canada*

Matthew Stuible − *Human Health Therapeutics, National Research Council Canada, Montreal, QC H4P 2R2, Canada*

Yves Durocher − *Human Health Therapeutics, National Research Council Canada, Montreal, QC H4P 2R2, Canada*

Jeremy E. Melanson − *Metrology, National Research Council Canada, Ottawa, ON K1A 0R6, Canada*

Complete contact information is available at: https://pubs.acs.org/10.1021/acsmeasuresciau.2c00050

Notes

The authors declare no competing financial interest.

ACKNOWLEDGMENTS

This work was supported by the NRC Pandemic Response Challenge Program. Juris Meija from NRC Metrology is acknowledged for assistance with stability data modeling.

REFERENCES

(1) *Johns Hopkins Coronavirus Resource Center*. https://coronavirus.jhu.edu (accessed 24 June 2022).

(2) Chi, X.; Yan, R.; Zhang, J.; Zhang, G.; Zhang, Y.; Hao, M.; Zhang, Z.; Fan, P.; Dong, Y.; Yang, Y.; Chen, Z.; Guo, Y.; Zhang, J.; Li, Y.; Song, X.; Chen, Y.; Xia, L.; Fu, L.; Hou, L.; Xu, J.; Yu, C.; Li, J.; Zhou, Q.; Chen, W. A neutralizing human antibody binds to the N-terminal domain of the Spike protein of SARS-CoV-2. *Science* **2020**, *369*, 650−655.

(3) Hansen, J.; Baum, A.; Pascal, K. E.; Russo, V.; Giordano, S.; Elzbieta Wloga, E.; Fulton, B. O.; Yan, Y.; Koon, K.; Patel, K.; Chung, K. M.; Hermann, A.; Ullman, E.; Cruz, J.; Rafique, A.; Huang, T.; Fairhurst, J.; Libertiny, C.; Malbec, M.; Lee, W.-Y.; Welsh, R.; Farr, G.; Pennington, S.; Deshpande, D.; Cheng, J.; Watty, A.; Bouffard, P.; Babb, R.; Levenkova, N.; Chen, C.; Zhang, B.; Romero Hernandez, A.; Saotome, K.; Zhou, Y.; Franklin, M.; Sivapalasingam, S.; Chien Lye, D.; Weston, S.; Logue, J.; Haupt, R.; Frieman, M.; Chen, G.; Olson, W.; Murphy, A. J.; Stahl, N.; Yancopoulos, G. D.; Kyratsous, C. A. Studies in humanized mice and convalescent humans yield a SARS-CoV-2 antibody cocktail. *Science* **2020**, *369*, 1010−1014.

(4) Cao, Y.; Wang, J.; Jian, F.; Xiao, T.; Song, W.; Yisimayi, A.; Huang, W.; Li, Q.; Wang, P.; An, R.; Wang, J.; Niu, X.; Yang, S.; Liang, H.; Sun, H.; Li, T.; Yu, Y.; Cui, Q.; Liu, S.; Yang, X.; Du, S.; Zhang, Z.; Hao, X.; Shao, F.; Jin, R.; Wang, X.; Xiao, J.; Wang, Y.; Sunney Xie, X. Omicron escapes the majority of existing SARS-CoV-2 neutralizing antibodies. *Nature* **2022**, *602*, 657−663.

(5) FDA Emergency Use Authorizations. https://www.fda.gov/medical-devices/coronavirus-disease-2019-covid-19-emergency-use-authorizations-medical-devices/in-vitro-diagnostics-euas (accessed 21 February 2022).

(6) Health Canada Authorized Medical Devices. https://www.canada.ca/en/health-canada/services/drugs-health-products/covid19-industry/medical-devices/authorized/list.html (accessed 21 February 2022).

(7) European Commission. *COVID-19 In Vitro Diagnostic Devices and Test Methods Database*. https://covid-19-diagnostics.jrc.ec.europa.eu/ (accessed 21 February 2022).
(8) Li, Y. H.; Li, J.; Liu, X. E.; Wang, L.; Li, T.; Zhou, Y. H.; Zhuang, H. Detection of the nucleocapsid protein of severe acute respiratory syndrome coronavirus in serum: comparison with results of other viral markers. *J. Virol. Methods* **2005**, *130*, 45−50.
(9) CDC. *Interim Guidelines for COVID-19 Antibody Testing*. https://www.cdc.gov/coronavirus/2019-ncov/lab/resources/antibody-tests-guidelines.html. Accessed: 01 June 2022.
(10) Beck, E. J.; Hsieh, Y. H.; Fernandez, R. E.; Dashler, G.; Egbert, E. R.; Truelove, S. A.; Garliss, C.; Wang, R.; Bloch, E. M.; Shrestha, R.; Blankson, J.; Cox, A. L.; Manabe, Y. C.; Kickler, T.; Rothman, R. E.; Redd, A. D.; Tobian, A. A.; Milstone, A. M.; Quinn, T. C.; Laeyendecker, O. Differentiation of SARS-CoV-2 naturally infected and vaccinated individuals in an inner-city emergency department. *medRxiv (Epidemiology)*, October 14, 2021, ver. 1. DOI: 10.1101/2021.10.13.21264968v1. (accessed 2022-07-12).
(11) Stocks, B. B.; Thibeault, M. P.; Schrag, J. D.; Melanson, J. E. Characterization of a SARS-CoV-2 Spike Protein Reference Material. *Anal. Bioanal. Chem.* **2022**, *414*, 3561−3569.
(12) Supekar, N. T.; Shajahan, A.; Gleinich, A. S.; Rouhani, D. S.; Heiss, C.; Chapla, D. G.; Moremen, K. W.; Azadi, P. Variable posttranslational modifications of severe acute respiratory syndrome coronavirus 2 nucleocapsid protein. *Glycobiology* **2021**, *31*, 1080−1092.
(13) Garcia-Cordero, J.; Mendoza-Ramirez, J.; Fernandez-Benavides, D.; Roa-Velazquez, D.; Filisola-Villasenor, J.; Martinez-Frias, S. P.; Sanchez-Salguero, E. S.; Miguel-Rodriguez, C. E.; Maravillas Montero, J. L.; Torres-Ruiz, J. J.; Gomez-Martin, D.; Argumedo, L. S.; Morales-Rios, E.; Alvarado-Orozco, J. M.; Cedillo-Barron, L. Recombinant Protein Expression and Purification of N, S1, and RBD of SARS-CoV-2 from Mammalian Cells and Their Potential Applications. *Diagnostics (Basel)* **2021**, *11*, 1808.
(14) de Camargo, B. R.; da Silva, L. A.; de Oliveira, A. S.; Ribeiro, B. M. An easy pipeline for one-step purification of SARS-CoV-2 nucleocapsid protein from insect cell suspension culture. *J. Virol. Methods* **2022**, *299*, 114341.
(15) Zeng, W.; Liu, G.; Ma, H.; Zhao, D.; Yang, Y.; Liu, M.; Mohammed, A.; Zhao, C.; Yang, Y.; Xie, J.; Ding, C.; Ma, X.; Weng, J.; Gao, Y.; He, H.; Jin, T. Biochemical characterization of SARS-CoV-2 nucleocapsid protein. *Biochem. Biophys. Res. Commun.* **2020**, *527*, 618−623.
(16) Colwill, K.; Galipeau, Y.; Stuible, M.; Gervais, C.; Arnold, C.; Rathod, B.; Abe, K. T.; Wang, J. H.; Pasculescu, A.; Maltseva, M.; Rocheleau, L.; Pelchat, M.; Fazel-Zarandi, M.; Iskilova, M.; Barrios-Rodiles, M.; Bennett, L.; Yau, K.; Cholette, F.; Mesa, C.; Li, A. X.; Paterson, A.; Hladunewich, M. A.; Goodwin, P. J.; Wrana, J. L.; Drews, S. J.; Mubareka, S.; McGeer, A. J.; Kim, J.; Langlois, M.-A.; Gingras, A.-C.; Durocher, Y. A scalable serology solution for profiling humoral immune responses to SARS-CoV-2 infection and vaccination. *Clin. Transl. Immunol.* **2022**, *11*, No. e1380.
(17) NRC Digital Repository. https://nrc-digital-repository.canada.ca/eng/search/?q=*&fc=%2Bcn%3Acrm&fc=%2Bsue%3Aamino+acid+standard&s=rcd (accessed 28 February 2022).
(18) Tyanova, S.; Temu, T.; Cox, J. The MaxQuant computational platform for mass spectrometry-based shotgun proteomics. *Nat. Protoc.* **2016**, *11*, 2301−2319.
(19) Schwanhausser, B.; Busse, D.; Li, N.; Dittmar, G.; Schuchhardt, J.; Wolf, J.; Chen, W.; Selbach, M. Global quantification of mammalian gene expression control. *Nature* **2011**, *473*, 337−342.
(20) Marty, M. T.; Baldwin, A. J.; Marklund, E. G.; Hochberg, G. K.; Benesch, J. L.; Robinson, C. V. Bayesian deconvolution of mass and ion mobility spectra: from binary interactions to polydisperse ensembles. *Anal. Chem.* **2015**, *87*, 4370−4376.
(21) Kou, Q.; Xun, L.; Liu, X. TopPIC: a software tool for top-down mass spectrometry-based proteoform identification and characterization. *Bioinformatics* **2016**, *32*, 3495−3497.
(22) Davidson, I. Hydrolysis of Samples for Amino Acid Analysis. In *Protein Sequencing Protocols*; Smith, B. J., Ed.; Humana Press: Totowa, NJ, 1997.
(23) Rutherford, S. M.; Gilani, G. S. Amino Acid Analysis. *Curr. Protoc. Protein Sci.* **2009**, *58*, 11.19.11−11.19.37.
(24) Pagliano, E.; Mester, Z.; Meija, J. Reduction of measurement uncertainty by experimental design in high-order (double, triple, and quadruple) isotope dilution mass spectrometry: application to GC-MS measurement of bromide. *Anal. Bioanal. Chem.* **2013**, *405*, 2879−2887.
(25) Josephs, R. D.; Li, M.; Daireaux, A.; Choteau, T.; Martos, G.; Westwood, S.; Wielgosz, R. I.; Li, H.; Wang, S.; Li, X.; Shi, N.; Wu, P.; Feng, L.; Huang, T.; Zhang, T.; Li, S.; Beltrão, P. J.; Marcos Saraiva, A.; Garrido, B. C.; Naressi Scapin, S. M.; Wollinger, W.; Bacila Sade, Y.; Thibeault, M.-P.; Stocks, B. B.; Melanson, J. E.; Kinumi, T.; Bin Rezali, M. F.; Öztug, M.; Akgöz, M.; Quaglia, M. Key Comparison Study on Peptide Purity - Synthetic Oxytocin. *Metrologia* **2020**, *57*, 08014.
(26) Josephs, R. D.; Li, M.; Song, D.; Westwood, S.; Stoppacher, N.; Daireaux, A.; Choteau, T.; Wielgosz, R. I.; Xiao, P.; Liu, Y.; Gao, X.; Zhang, C.; Zhang, T.; Mi, W.; Quan, C.; Huang, T.; Li, H.; Flatschart, R.; Borges Oliveira, R.; Melanson, J. E.; Ohlendorf, R.; Henrion, A.; Kinumi, T.; Wong, L.; Liu, Q.; Oztug Senal, M.; Vatansever, B.; Ün, I.; Gören, A. C.; Akgöz, M.; Quaglia, M.; Warren, J. Key Comparison Study on Peptide Purity - Synthetic Human C-peptide. *Metrologia* **2017**, *54*, 08007.
(27) Mi, W.; Josephs, R. D.; Melanson, J. E.; Dai, X.; Wang, Y.; Zhai, R.; Chu, Z.; Fang, X.; Thibeault, M.-P.; Stocks, B. B.; Meija, J.; Bedu, M.; Martos, G.; Westwood, S.; Wielgosz, R. I.; Liu, Q.; Teo, T. L.; Liu, H.; Tan, Y. J.; Öztug, M.; Saban, E.; Kinumi, T.; Saikusa, K.; Schneider, R. J.; Weller, M. G.; Konthur, Z.; Jaeger, C.; Quaglia, M.; Mussell, C.; Drinkwater, G.; Giangrande, C.; Vaneeckhoutte, H.; Boeuf, A.; Delatour, V.; Lee, J. E.; O'Connor, G.; Ohlendorf, R.; Henrion, A.; Beltrão, P. J.; Naressi Scapin, S. M.; Sade, Y. B. PAWG Pilot Study on Quantification of SARS-CoV-2 Monoclonal Antibody - Part 1. *Metrologia* **2022**, *59*, 08001.
(28) Liu, J.; Zhu, W.; Sun, H.; Song, D.; Xiao, P.; Xu, B.; Li, H. Development of a primary reference material of natural C-reactive protein: verification of its natural pentameric structure and certification by two isotope dilution mass spectrometry. *Anal. Methods* **2021**, *13*, 626−635.
(29) Wang, X.; Wu, L.; Huang, Y.; Su, P.; Yang, Y.; Yang, B.; Zhang, N. Development of a human insulin certified reference material with SI-traceable purity. *Anal. Bioanal. Chem.* **2022**, *414*, 3443.
(30) Pace, C. N.; Vajdos, F.; Fee, L.; Grimsley, G.; Gray, T. How to measure and predict the molar absorption coefficient of a protein. *Protein Sci.* **1995**, *4*, 2411−2423.
(31) Krokhin, O.; Li, Y.; Andonov, A.; Feldmann, H.; Flick, R.; Jones, S.; Stroeher, U.; Bastien, N.; Dasuri, K. V. N.; Cheng, K.; Simonsen, J. N.; Perreault, H.; Wilkins, J.; Ens, W.; Plummer, F.; Standing, K. G. Mass Spectrometric Characterization of Proteins from the SARS Virus. *Mol. Cell. Proteomics* **2003**, *2*, 346−356.
(32) Ying, W.; Hao, Y.; Zhang, Y.; Peng, W.; Qin, E.; Cai, Y.; Wei, K.; Wang, J.; Chang, G.; Sun, W.; Dai, S.; Li, X.; Zhu, Y.; Li, J.; Wu, S.; Guo, L.; Dai, J.; Wang, J.; Wan, P.; Chen, T.; Du, C.; Li, D.; Wan, J.; Kuai, X.; Li, W.; Shi, R.; Wei, H.; Cao, C.; Yu, M.; Liu, H.; Dong, F.; Wang, D.; Zhang, X.; Qian, X.; Zhu, Q.; He, F. Proteomic analysis on structural proteins of Severe Acute Respiratory Syndrome coronavirus. *Proteomics* **2004**, *4*, 492−504.
(33) Technical Committee ISO/REMCO. *ISO Guide 35:2017. Reference Materials—Guidance for Characterization and Assessment of Homogeneity and Stability*; International Organization for Standardization, 2017.
(34) Cong, Y.; Kriegenburg, F.; de Haan, C. A. M.; Reggiori, F. Coronavirus nucleocapsid proteins assemble constitutively in high molecular oligomers. *Sci. Rep.* **2017**, *7*, 5740.
(35) Ye, Q.; West, A. M. V.; Silletti, S.; Corbett, K. D. Architecture and self-assembly of the SARS-CoV-2 nucleocapsid protein. *Protein Sci.* **2020**, *29*, 1890−1901.

(36) Luo, H.; Chen, J.; Chen, K.; Shen, X.; Jiang, H. Carboxyl Terminus of Severe Acute Respiratory Syndrome Coronavirus Nucleocapsid Protein: Self-Association Analysis and Nucleic Acid Binding Characterization. *Biochemistry* **2006**, *45*, 11827−11835.
(37) Stocks, B. B.; Thibeault, M.-P.; L'Abbé, D.; Gervais, C.; Pelletier, A.; Stuible, M.; Durocher, Y.; Melanson, J. E. *NCAP-1: SARS-CoV-2 Nucleocapsid Protein Reference Material*; National Research Council Canada: Ottawa, 2021. .
(38) Arya, R.; Kumari, S.; Pandey, B.; Mistry, H.; Bihani, S. C.; Das, A.; Prashar, V.; Gupta, G. D.; Panicker, L.; Kumar, M. Structural insights into SARS-CoV-2 proteins. *J. Mol. Biol.* **2021**, *433*, 166725.
(39) Meyer, B.; Chiaravalli, J.; Gellenoncourt, S.; Brownridge, P.; Bryne, D. P.; Daly, L. A.; Grauslys, A.; Walter, M.; Agou, F.; Chakrabarti, L. A.; Craik, C. S.; Eyers, C. E.; Eyers, P. A.; Gambin, Y.; Jones, A. R.; Sierecki, E.; Verdin, E.; Vignuzzi, M.; Emmott, E. Characterising proteolysis during SARS-CoV-2 infection identifies viral cleavage sites and cellular targets with therapeutic potential. *Nat. Commun.* **2021**, *12*, 5553.
(40) Lutomski, C. A.; El-Baba, T. J.; Bolla, J. R.; Robinson, C. V. Multiple Roles of SARS-CoV-2 N Protein Facilitated by Proteoform-Specific Interactions with RNA, Host Proteins, and Convalescent Antibodies. *JACS Au* **2021**, *1*, 1147−1157.
(41) Wu, C.; Qavi, A. J.; Hachim, A.; Kavian, N.; Cole, A. R.; Moyle, A. B.; Wagner, N. D.; Sweeney-Gibbons, J.; Rohrs, H. W.; Gross, M. L.; Peiris, J. S. M.; Basler, C. F.; Farnsworth, C. W.; Valkenburg, S. A.; Amarasinghe, G. K.; Leung, D. W. Characterization of SARS-CoV-2 nucleocapsid protein reveals multiple functional consequences of the C-terminal domain. *iScience* **2021**, *24*, 102681.
(42) Tugaeva, K. V.; Hawkins, D. E. D. P.; Smith, J. L. R.; Bayfield, O. W.; Ker, D.-S.; Sysoev, A. A.; Klychnikov, O. I.; Antson, A. A.; Sluchanko, N. N. The Mechanism of SARS-CoV-2 Nucleocapsid Protein Recognition by the Human 14−3-3 Proteins. *J. Mol. Biol.* **2021**, *433*, 166875.
(43) Nikolakaki, E.; Giannakouros, T. SR/RS Motifs as Critical Determinants of Coronavirus Life Cycle. *Front. Mol. Biol.* **2020**, *7*, 219.
(44) Mark, J.; Li, X.; Cyr, T.; Fournier, S.; Jaentschke, B.; Hefford, M. A. SARS coronavirus: Unusual lability of the nucleocapsid protein. *Biochem. Biophys. Res. Commun.* **2008**, *377*, 429−433.
(45) Tylor, S.; Andonov, A.; Cutts, T.; Cao, J.; Grudesky, E.; Van Domselaar, G.; Li, X.; He, R. The SR-rich motif in SARS-CoV nucleocapsid protein is important for virus replication. *Can. J. Microbiol.* **2009**, *55*, 254−260.
(46) Lin, L.; Shao, J.; Sun, M.; Liu, J.; Xu, G.; Zhang, X.; Xu, N.; Wang, R.; Liu, S. Identification of phosphorylation sites in the nucleocapsid protein (N protein) of SARS-coronavirus. *Int. J. Mass Spectrom.* **2007**, *268*, 296−303.
(47) Rump, A.; Risti, R.; Kristal, M. L.; Reut, J.; Syritski, V.; Lookene, A.; Ruutel Boudinot, S. Dual ELISA using SARS-CoV-2 nucleocapsid protein produced in E. coli and CHO cells reveals epitope masking by N-glycosylation. *Biochem. Biophys. Res. Commun.* **2021**, *534*, 457−460.
(48) Nie, S.; Greer, T.; O'Brien Johnson, R.; Zheng, X.; Torri, A.; Li, N. Simple and Sensitive Method for Deep Profiling of Host Cell Proteins in Therapeutic Antibodies by Combining Ultra-Low Trypsin Concentration Digestion, Long Chromatographic Gradients, and BoxCar Mass Spectrometry Acquisition. *Anal. Chem.* **2021**, *93*, 4383−4390.
(49) He, H. J.; Stein, E. V.; DeRose, P.; Cole, K. D. Limitations of methods for measuring the concentration of human genomic DNA and oligonucleotide samples. *Biotechniques* **2018**, *64*, 59−68.
(50) Quadeer, A. A.; Ahmed, S. F.; McKay, M. R. Landscape of epitopes targeted by T cells in 852 individuals recovered from COVID-19: Meta-analysis, immunoprevalence, and web platform. *Cell Rep. Med.* **2021**, *2*, 100312.
(51) Taus, E.; Hofmann, C.; Ibarrondo, F. J.; Hausner, M. A.; Fulcher, J. A.; Krogstad, P.; Ferbas, K. G.; Tobin, N. H.; Rimoin, A. W.; Aldrovandi, G. M.; Yang, O. O. Dominant $CD8^+$ T Cell Nucleocapsid Targeting in SARS-CoV-2 Infection and Broad Spike Targeting From Vaccination. *Front. Immunol.* **2022**, *13*, 835830.
(52) Phatarphekar, A.; Vidyadhar Reddy, G. E. C.; Gokhale, A.; Karanam, G.; Kuchroo, P.; Shinde, K.; Masand, G.; Pagare, S.; Khadpe, N.; Pai, S. S.; Vijayan, V.; Ramnath, R. L.; Reddy, K. P.; Rao, P.; Rao, S. H.; Ramana, V. RelCoVax®, a two antigen subunit protein vaccine candidate against SARS-CoV-2 induces immune responses in mice. *Vaccine* **2022**, *40*, 4522−4530.
(53) Afkhami, S.; D'Agostino, M. R.; Zhang, A.; Stacey, H. D.; Marzok, A.; Kang, A.; Singh, R.; Bavananthasivam, J.; Ye, G.; Luo, X.; Wang, F.; Ang, J. C.; Zganiacz, A.; Sankar, U.; Kazhdan, N.; Koenig, J. F. E.; Phelps, A.; Gameiro, S. F.; Tang, S.; Jordana, M.; Wan, Y.; Mossman, K. L.; Jeyanathan, M.; Gillgrass, A.; Medina, M. F. C.; Smaill, F.; Lichty, B. D.; Miller, M. S.; Xing, Z. Respiratory mucosal delivery of next-generation COVID-19 vaccine provides robust protection against both ancestral and variant strains of SARS-CoV-2. *Cell* **2022**, *185*, 896−915.
(54) Stuible, M.; van Lier, F.; Croughan, M. S.; Durocher, Y. Beyond preclinical research: production of CHO-derived biotherapeutics for toxicology and early-phase trials by transient gene expression or stable pools. *Curr. Op. Chem. Eng.* **2018**, *22*, 145−151.

https://doi.org/10.1021/acsmeasuresciau.2c00050
ACS Meas. Sci. Au 2022, 2, 620−628